

SUPPLEMENTAL MATERIAL

Endothelial cell transforming growth factor- β signaling regulates venous adaptive remodeling to improve arteriovenous fistula patency

Ryosuke Taniguchi (谷口良輔),^{1,2} Yuichi Ohashi (大橋雄一),^{1,2} Jung Seok Lee (이중석),³
Haidi Hu (胡海地),^{1,4} Luis Gonzalez,¹ Weichang Zhang (张惟常),¹ John Langford,¹
Yutaka Matsubara (松原裕),^{1,5} Bogdan Yatsula,¹ George Tellides,^{1,6,8}
Tarek M. Fahmy,³ Katsuyuki Hoshina (保科克行),² Alan Dardik^{1,7,8}

1. Vascular Biology and Therapeutics Program, Yale School of Medicine, New Haven, CT
2. Division of Vascular Surgery, The University of Tokyo, Bunkyo-ku, Tokyo, Japan
3. Department of Biomedical Engineering, Yale University, New Haven, CT
4. Department of Vascular and Thyroid Surgery, the First Hospital of China Medical University, Shenyang, China
5. Department of Surgery and Sciences, Kyushu University, Fukuoka, Japan
6. Division of Cardiac Surgery, Department of Surgery, Yale School of Medicine, New Haven, CT
7. Division of Vascular and Endovascular Surgery, Department of Surgery, Yale School of Medicine, New Haven, CT
8. Department of Surgery, VA Connecticut Healthcare Systems, West Haven, CT

TABLE OF CONTENTS

- 1. Supplemental Methods.**
- 2. Supplemental Results.**
- 3. Table S1.** Major resources.
- 4. Figure S1.** Study design.
- 5. Figure S2.** Expression of TGF- β 1, p-Smad2 and Smad2 in the arteriovenous fistula (AVF) wall in male mice.
- 6. Figure S3.** Expression of TGF- β 1, p-Smad2 and Smad2 in the arteriovenous fistula (AVF) wall in female mice
- 7. Figure S4.** Activation of Smad2 by arterial shear stress is inhibited by SB431542.
- 8. Figure S5.** Enhanced retention of nanoparticles (NP) in vivo.
- 9. Figure S6.** Immunofluorescence (IF) microscopy in mice treated with Rhodamine B-containing nanoparticles in pluronic gel.
- 10. Figure S7.** Controlled release of SB431542-containing nanoparticles in vitro.
- 11. Figure S8.** SB431542-containing nanoparticles (NP-SB) do not alter outward remodeling of the vessels and flow dynamics of the inflow aorta.
- 12. Figure S9.** SB431542-containing nanoparticles (NP-SB) do not impact the expression of PDGF-B and FGF-2.
- 13. Figure S10.** Confirmation of Cre recombination with tamoxifen in TGF- β receptor knock out mice.
- 14. Figure S11** Inhibition of TGF- β signaling in smooth muscle cells.
- 15. Figure S12** Inhibition of TGF- β signaling in smooth muscle cells.
- 16. Figure S13.** Inhibition of TGF- β signaling in endothelial cells.
- 17. Figure S14.** Inhibition of TGF- β signaling in endothelial cells.
- 18. Figure S15.** Summary of the effect of pharmacological pan-inhibition and cell type-specific inhibition of TGF- β signaling on AVF maturation.

SUPPLEMENTAL METHODS

Cell Culture

Primary mouse lung EC were prepared and cultured as described previously.^{13,52} The sex of EC used was not determined. Briefly, EC were cultured in endothelial basal medium 2 with Endothelial Cell Growth Media-2 MV SingleQuot Kit Supplement and Growth Factors (Lonza), 20% fetal bovine serum (Gibco) and 1% penicillin/streptomycin (Gibco), 2 mmol/L L-glutamine (Corning Life Sciences).

In Vitro Smad2 Manipulation

EC at 80% confluence in 6-well plates were serum-starved for 12 hours and then stimulated with TGF β 1 (5 ng/ml) with or without cotreatment with SB431542 (10 μ M) in EBM-2 medium without any growth factors or FBS. After treatment (1 hour), 6-well plates were washed twice with cold PBS, EC were removed with radioimmunoprecipitation assay lysis buffer (Beyotime), and cell lysate extracted for further study.

Laminar Shear Stress Treatment

EC were seeded and cultured on collagen 1-coated glass plates (StreamerTM Culture Slips, Flexcell Corporation) until ~80% confluent and then serum-starved for 24 hours. In some experiments, the EC were pretreated with SB431542 (10 μ M) or vehicle for 1 hour in an incubator (37°C, 5%CO₂). EC were exposed to laminar shear stress using a parallel-plate flow chamber with circulating Endothelial Basal Media-2 medium (0% fetal bovine serum, 37 \pm 0.5°C), as described previously.^{13,52} The magnitude of shear stress was set at 0, 3, or 20 dynes/cm². After 1 hour of shear stress treatment, slides were washed twice with cold PBS, EC were removed with radioimmunoprecipitation assay lysis buffer, and cell lysate extracted for further study.

Synthesis and characterization of nanoparticles

Nanoparticles were made encapsulating Rhodamine B (Sigma-Aldrich) or SB431542 (Abcam); Poly(lactic-co-glycolic acid) nanoparticles were prepared with an established emulsion method.⁵³⁻⁵⁵ Briefly, Poly(lactic-co-glycolic acid) (100 mg, inherent viscosity 0.55-0.75 dL/g, ester terminal) and encapsulant (SB431542, 20 mg; Rhodamine B, 20 mg) were dissolved in chloroform, and then added drop-wise to 5% poly(vinyl alcohol) (Sigma-Aldrich). The mixture was sonicated 3 times and then added to 0.2% poly(vinyl alcohol) solution. The solvent was evaporated for 2 hours under stirring and the poly(lactic-co-glycolic acid) particles were centrifuged before lyophilization. Concentrations of SB431542 and Rhodamine B were determined by

spectrophotometry (SpectraMax M5, Molecular Devices) at 320 and 565 nm, respectively. Pluronic F-127 (Sigma-Aldrich) was dissolved in PBS (30 wt%) for 3 days at 4°C and the nanoparticles were added (50 mg particles/mL, 50 µg SB/mg NP [25% loading efficiency]). SB431542-containing nanoparticles are hereafter referred to as NP-SB.

Imaging of Rhodamine B-containing nanoparticles

Rhodamine B-containing nanoparticles (NP-RhB) were dissolved in pluronic gel and applied to the adventitia of the AVF prior to closing the abdomen (200 µl/mice). At various time points, the fluorescence intensity in the whole body of post-operative mice were evaluated with an in-vivo imaging system (IVIS [In-Vivo MS FX PRO, Bruker, Billerica, MA]) under general anesthesia using 2% to 3% isoflurane. The same set of mice were serially examined for the whole body IVIS imaging. For the ex-vivo IVIS imaging, mice treated with NP-RhB were euthanized at different time points. Subsequently, several organs were harvested, and the fluorescence intensity was evaluated with IVIS. To premeasure the autofluorescence of the whole body or each organ, mouse models without NP-RhB administration were prepared in the same manner. Organs were embedded in OCT (Tissue-Tek) and preserved in -80°C for immunofluorescence studies. Images obtained with IVIS were subjected to interpretation on Bruker Molecular Imaging Software 7.5 for evaluation and quantification. The fluorescence images were merged with X-ray images of the mice.

Kinetic analysis of SB431542-containing nanoparticles

SB431542-containing nanoparticles (NP-SB) in pluronic gel were placed in a microdialysis system and the release of SB431542 was monitored by periodic withdrawal of PBS samples. This was also performed with NP-SB without pluronic gel. The release was studied by placing a dispersion of NP-SB into a dialysis bag (cut-off 20,000 g/mol, Millipore) and immersing the bag into a vial containing PBS (1% Tween, 10 mL). At appropriate times, 1 ml of the release medium was collected from the vials and the medium was replaced by fresh PBS.

SUPPLEMENTAL RESULTS

Phosphorylation of Smad2 by arterial shear stress is inhibited by SB431542

Since Smad2 is phosphorylated in the remodeling AVF wall (**Figure 1**), and our data suggest that this may occur in EC, we determined whether Smad2 could be phosphorylated in EC *in vitro*. Mouse EC were stimulated with TGF- β 1 under static conditions that increased Smad2 phosphorylation and phosphorylation was diminished with SB431542, an inhibitor of TGF- β receptor I (**Figure S4A**). Since AVF are characterized by increased magnitudes of shear stress on the EC,⁵⁶⁻⁵⁸ we determined whether arterial magnitudes of shear stress could phosphorylate Smad2 in EC. Mouse EC were treated with different magnitudes of shear stress; arterial (20 dyne/cm²) magnitudes of shear stress increased Smad2 phosphorylation compared to static (0 dyne/cm²) or venous (3 dyne/cm²) magnitudes of shear stress (**Figure S4B**), and this increase in Smad2 phosphorylation was diminished with pretreatment with SB431542 (**Figure S4B**). These data show that SB431542 inhibits Smad2 phosphorylation in EC *in vitro*.

Enhanced retention of nanoparticles (NP) *in vivo*

Prior to SB431542 treatment, we examined nanoparticles containing Rhodamine B, a fluorescent marker, to trace nanoparticles *in vivo*. Rhodamine B-containing nanoparticles (NP-RhB) were dissolved in pluronic gel and applied to the AVF adventitia just after surgical creation of the fistula and prior to closing the abdomen. Observation of mice with IVIS imaging showed that Rhodamine B fluorescence was rapidly and easily detectable within 2 hours of surgery and then decreased steeply in the first 2 days but was detectable for at least 7 days (**Figure S5A, B**). We next harvested several organs of mice treated with NP-RhB at several postoperative time points and examined Rhodamine B fluorescence; all organs including the AVF showed increased fluorescence at postoperative day 1 (**Figure S5C, D**). In the AVF and the heart, fluorescence declined to baseline by day 14 (**Figure S5C, D**; black and purple); however, increased fluorescence was sustained through day 14 in the liver, spleen, kidney, lung and the gastrointestinal tract (**Figure S5C, D**; blue, green, magenta, orange and red). In the AVF, Rhodamine B was observed on or slightly beneath the retroperitoneal surface but was not easily detectable in the AVF wall at day 1 (**Figure S6A**). In the liver and the spleen, Rhodamine B was detectable in the organ parenchyma at day 1 (**Figure S6B**); in the kidney, Rhodamine B was observed on the surface but was not detectable in the parenchyma at day 1 (**Figure S6B**). These data show that NP-RhB is detectable in mice for at least 2 weeks with a single dose delivered to the

adventitia at the time of surgery, suggesting the utility of nanoparticle-based drug delivery.

Controlled release of SB431542-containing nanoparticles

Nanoparticles containing SB431542 (NP-SB) were synthesized in the same manner as NP-RhB. The pharmacokinetics of SB431542 release from NP-SB was assessed *in vitro*; cumulative release of SB431542 was sustained for at least 21 days (**Figure S7A**; black). In addition, NP-SB that were dissolved in pluronic gel showed less cumulative release of SB431542, with approximately 60% by day 21 (**Figure S7A**; blue).

Table S1. Major Resources**Animals (in vivo studies)**

Species	Vendor or Source	Background Strain	Sex	Persistent ID / URL
C57BL/6J Mouse	The Jackson Laboratory	C57BL/6J	Male	Stock No: 000664
C57BL/6J Mouse	The Jackson Laboratory	C57BL/6J	Female	Stock No: 000664

Antibodies

Target antigen	Vendor or Source	Catalog #	Working concentration	Persistent ID / URL
Phospho-Akt1	Cell Signaling	9018	10 µg/ml	https://www.cellsignal.com/products/primary-antibodies/phospho-akt1-ser473-d7f10-xp-rabbit-mab-akt1-specific/9018
α-SMA	Abcam	ab7817	5 µg/mL	https://www.abcam.com/alpha-smooth-muscle-actin-antibody-1a4-ab7817.html
CD206	Abcam	ab64693	5 µg/ml	https://www.abcam.com/mannose-receptor-antibody-ab64693.html
CD3	R&D systems	MAB4841	25 µg/ml	https://www.rndsystems.com/products/mouse-cd3-antibody-17a2_mab4841
CD4	Abcam	ab183685	10 µg/ml	https://www.abcam.com/cd4-antibody-epr19514-ab183685.html
CD68	Bio-Rad	MCA1957	10 µg/ml	https://www.bio-rad-antibodies.com/monoclonal/mousecd68-antibody-fa-11-mca1957.html?f=purified
CD8	Abcam	ab203035	10 µg/ml	https://www.abcam.com/cd8-antibody-ab203035.html
CD90	BD Biosciences	553016	10 µg/ml	https://www.bdbiosciences.com/en-us/products/reagents/flow-cytometry-reagents/research-reagents/single-color-antibodies-ruo/purified-rat-anti-mouse-cd90.553016
Cleaved Caspase-3	Cell Signaling	9664	0.2 µg/ml	https://www.cellsignal.com/products/primary-antibodies/cleaved-caspase-3-asp175-5a1e-rabbit-mab/9664
Collagen I	Abcam	ab34710	5 µg/ml	https://www.abcam.com/collagen-i-antibody-ab34710.html

Collagen III	Abcam	ab7778	5 µg/ml	https://www.abcam.com/collagen-iii-antibody-ab7778.html
FGF-2	BioLegend	A15021A	5 µg/ml	https://www.biolegend.com/en-us/products/purified-anti-fgf-basic-antibody-13445?GroupID=GROUP26
Fibronectin	Abcam	ab2413	8 µg/ml	https://www.abcam.com/fibronectin-antibody-ab2413.html
Foxp3	Abcam	ab212700	5 µg/ml	https://www.abcam.com/foxp3-antibody-3g3-bsa-andazide-free-ab212700.html
GAPDH	Cell Signaling	2118	1 µg/ml	https://www.cellsignal.com/products/primary-antibodies/gapdh-14c10-rabbit-mab/2118
ICAM-1	R&D systems	AF796	2 µg/mL	https://www.rndsystems.com/products/mouse-icam-1-cd54-antibody_af796
IFN γ -R	Abcam	ab77246	10 µg/ml	https://www.abcam.com/ifn-gamma-receptor-betaaf-1-antibody-ab77246.html
IL-10	Abcam	ab9969	10 µg/ml	HTTPS://WWW.ABCAM.COM/IL-10-ANTIBODY-AB9969.HTML
iNOS	Abcam	ab15323	10 µg/ml	https://www.abcam.com/inos-antibody-ab15323.html
Myh10	Abcam	ab230823	0.6 µg/ml	HTTPS://WWW.ABCAM.COM/NON-MUSCLE-MYOSIN-IIBMYH10-ANTIBODY-EPR22564-23-AB230823.HTML
Myh11	Abcam	ab683	0.5 µg/ml	https://www.abcam.com/smooth-muscle-myosin-heavy-chain-11-antibody-1g12-ab683.html
N-cadherin	Abcam	ab18203	10 µg/ml	https://www.abcam.com/n-cadherin-antibody-intercellular-junction-marker-ab18203.html
PCNA	DAKO	M0879	1.6 µg/mL	https://www.chem.agilent.com/store/productDetail.jsp?catalogId=M087901-2&catId=SubCat3ECS_86416
PDGF-B	Santa Cruz	sc7878	2 µg/mL	https://www.scbt.com/p/pdgf-b-antibody-h-55?productCanUrl=pdgf-b-antibody-h-55&requestid=1836568
Smad2	Cell Signaling	5339	3 µg/mL	https://www.cellsignal.com/products/primary-antibodies/smad2-d43b4-xp-rabbit-mab/5339

Phospho-Smad2	Sigma-Aldrich	AB3849-I	5 µg/ml	https://www.emdmillipore.com/US/en/product/Anti-phospho-SMAD2-Antibody-Ser465-467,MM_NF-AB3849-I
Phospho-Smad3	Abcam	ab52903	11.5 µg/ml	https://www.abcam.com/smad3-phospho-s423--s425-antibody-ep823y-ab52903.html
TAK1	Invitrogen	PA5-20083	20 µg/ml	https://www.thermofisher.com/antibody/product/TAK1-Antibody-Polyclonal/PA5-20083
TGF-β1	Abcam	ab92486	5 µg/mL	https://www.abcam.com/tgf-beta-1-antibody-ab92486.html
TGM2	Cell Signaling	3557	10 µg/ml	https://www.cellsignal.com/products/primary-antibodies/tgm2-d11a6-xp-rabbit-mab/3557
Vimentin	Abcam	ab45939	2 µg/mL	https://www.abcam.com/vimentin-antibody-cytoskeleton-marker-ab45939.html
HRP-linked anti-rabbit IgG	Cell Signaling	7074	0.5 µg/ml	https://www.cellsignal.com/products/secondaryantibodies/anti-rabbit-igg-hrp-linked-antibody/7074

Cultured Cells

Name	Vendor or Source	Sex (F, M, or unknown)	Persistent ID / URL
Primary mouse lung endothelial cells	Isolated from 3-4 pairs of lungs dissected from mice between 3-4 weeks of age	Unknown	

Other

Description	Source / Repository	Persistent ID / URL
Tamoxifen	Sigma-Aldrich	T5648; https://www.sigmaaldrich.com/catalog/product/sigma/t5648
SB431542	Abcam	ab120163; https://www.abcam.com/sb431542-alk-inhibitor-ab120163.html
Rhodamine B	Sigma-Aldrich	R6626; https://www.sigmaaldrich.com/catalog/product/sigma/r6626
Pluronic® F-127	Sigma-Aldrich	P2443; https://www.sigmaaldrich.com/catalog/product/sigma/p2443
Poly(vinyl alcohol) (PVA)	Sigma-Aldrich	360627; https://www.sigmaaldrich.com/catalog/product/aldrich/360627

Poly(lactic-co-glycolic acid) (PLGA)	Durect	B6010-2; https://www.absorbables.com/products/plga/
--------------------------------------	--------	--

Figure S1

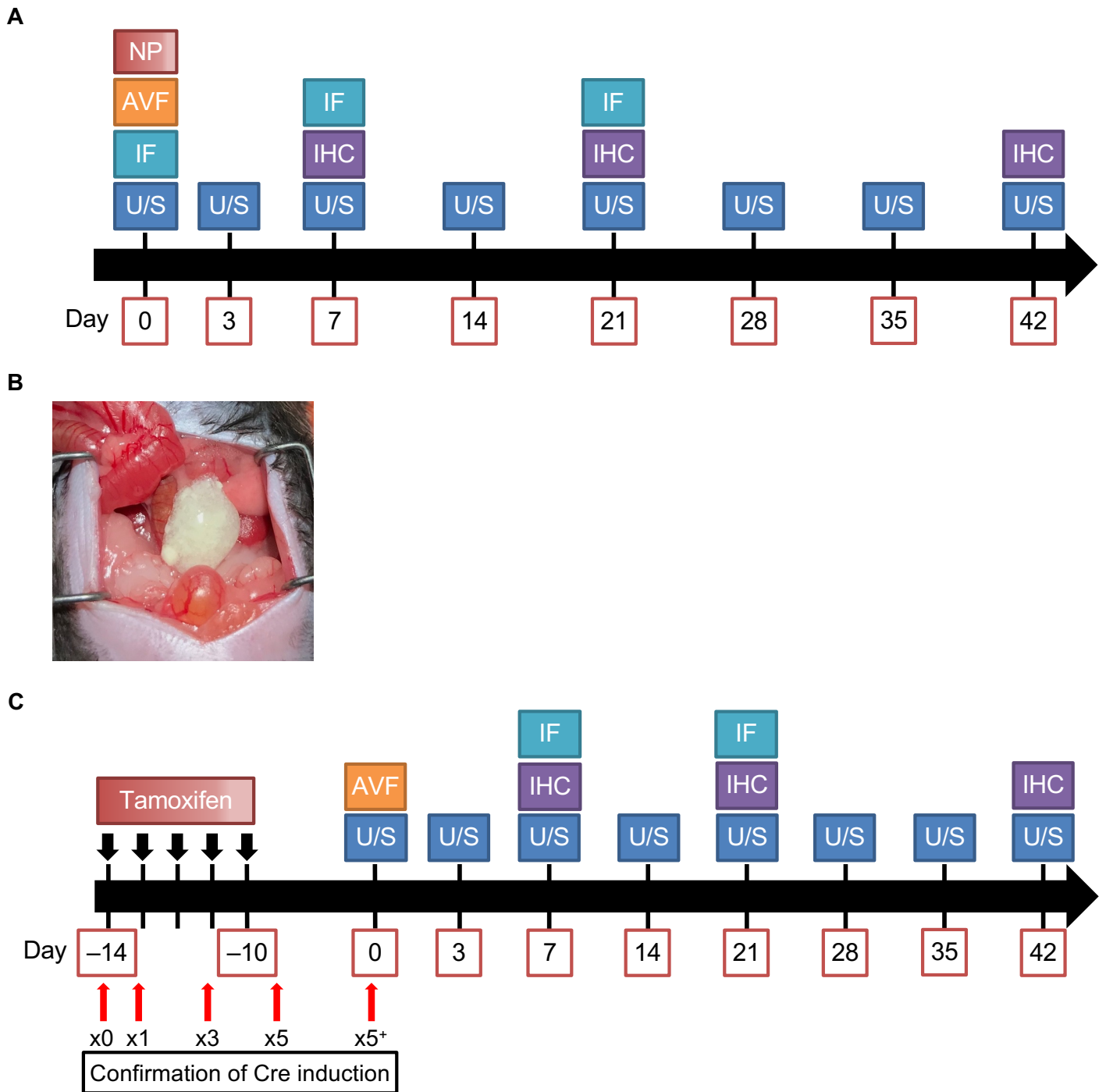


Figure S1. Study design. (A) Flow chart showing the experimental design of study examining the effect of SB431542-containing nanoparticles (NP-SB). Mice received single periaortic application of NP-SB (20 mg SB/kg) or unloaded nanoparticles (NP-control) during AVF creation (Day 0). (B) Operative photograph showing periaortic application of NP-SB in pluronic gel. (C) Flow chart showing the experimental design of study with inducible TGF- β receptor knock out mice. Mice were intraperitoneally injected with 2mg of tamoxifen or vehicle (corn oil) daily for 5 consecutive days, starting at 14 days prior to arteriovenous fistula (AVF) creation (day 0). To confirm adequate Cre induction with tamoxifen, the inferior vena cava (IVC) was harvested prior to injection (x0) or a day after 1, 3, 5 injections (x1, x3, x5, respectively). Additionally, the IVC was harvested 14 days from the start of the injections (x5⁺) when the mice would undergo AVF creation. AVF, AVF creation; IF, immunofluorescence; IHC, immunohistochemistry; NP, nanoparticle application; U/S, ultrasound.

Figure S2

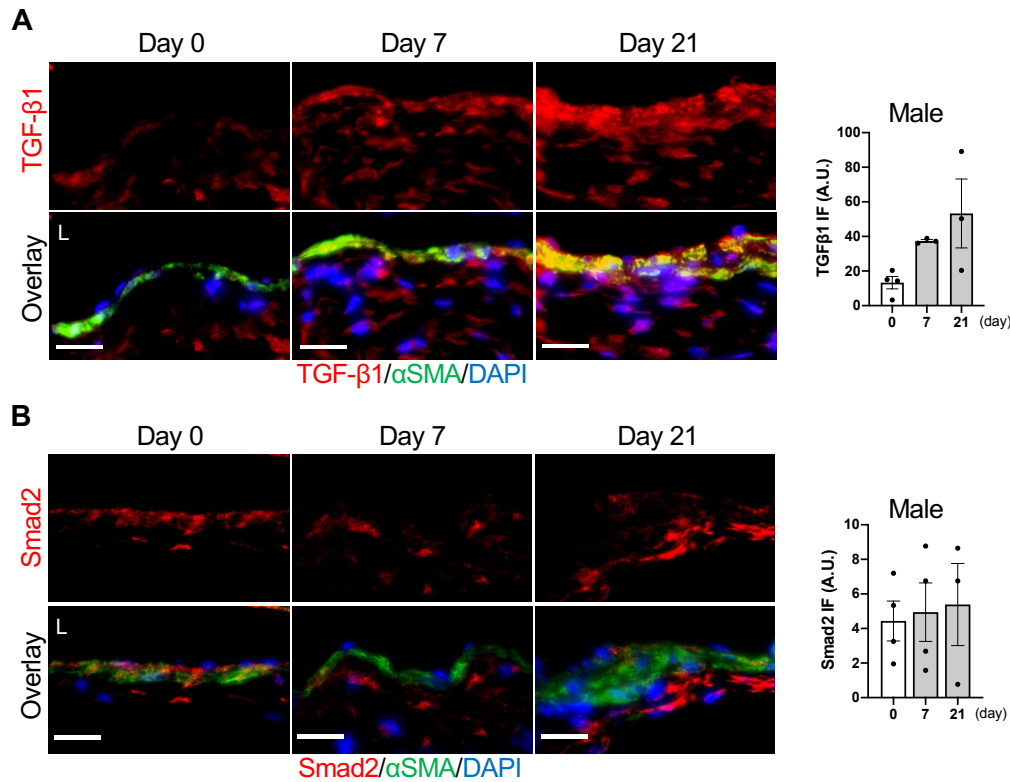


Figure S2. Expression of TGF-β1 and Smad2 in the arteriovenous fistula (AVF) wall in male mice. (A, B) Representative photomicrographs of the AVF wall in male mice (days 0 to 21) showing immunofluorescence (IF) of (A) TGF-β1 (red), αSMA (green) and DAPI (blue) quantified as IF intensity of TGF-β1 in the AVF wall; $P=0.0718$ (ANOVA), $P=0.0533$ (Kruskal-Wallis). (B) Smad2 (red), αSMA (green) and DAPI (blue) quantified as IF intensity of Smad2 in the AVF wall; $P=0.9280$ (ANOVA), $P=0.9934$ (Kruskal-Wallis); $n=4$ (days 0 and 7) and 3 (day 21). Four high power field images were used to acquire the mean value per animal. All data are represented as mean value \pm SEM. L, lumen; A.U., arbitrary unit. Scale bars, 20 μ m.

Figure S3

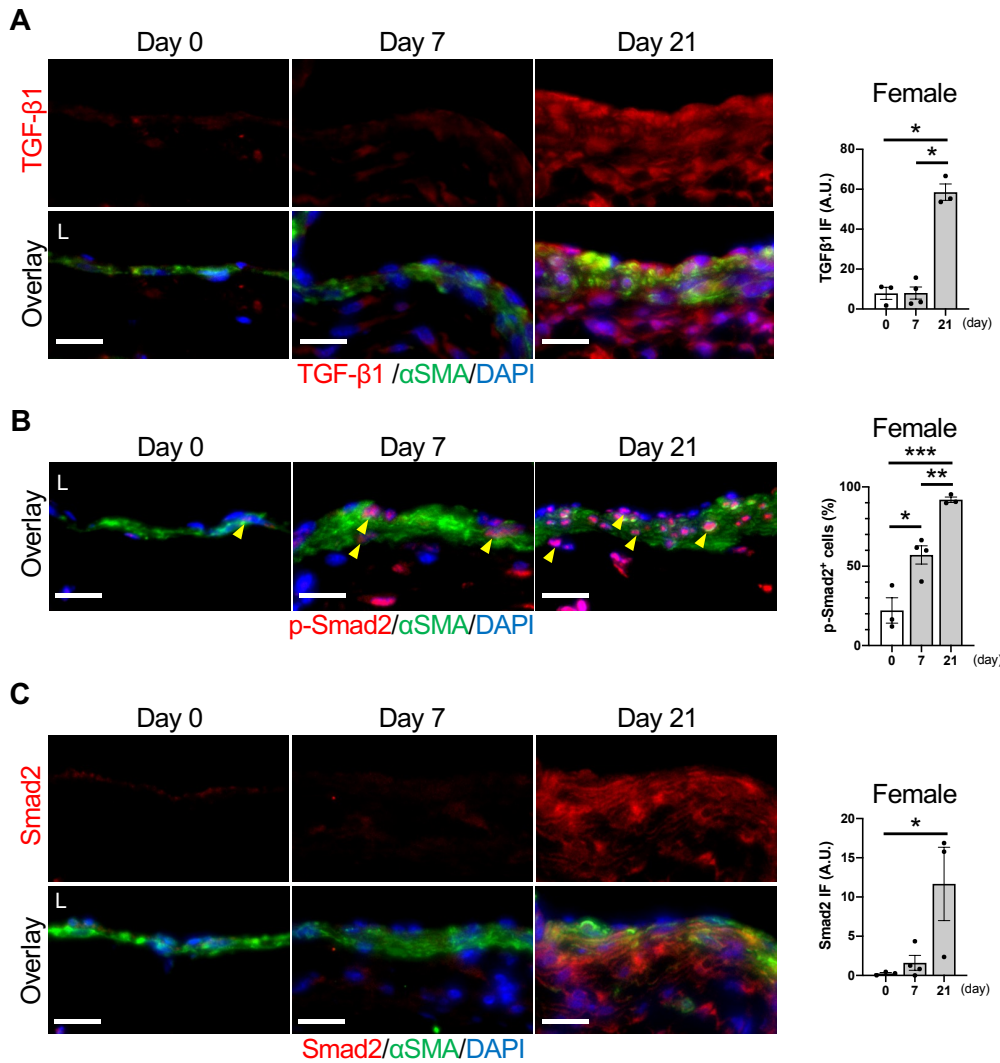


Figure S3. Expression of TGF-β1, p-Smad2 and Smad2 in the arteriovenous fistula (AVF) wall in female mice. (A-C) Representative photomicrographs of the AVF wall in female mice (days 0 to 21) showing IF of **(A)** TGF-β1 (red), αSMA (green) and DAPI (blue) quantified as IF intensity of TGF-β1 in the AVF wall; $P < 0.0001$ (ANOVA), $P = 0.0505$ (Kruskal-Wallis), $*P < 0.0001$ (day 0 vs 21, day 7 vs 21, Tukey's post hoc). **(B)** p-Smad2 (red), αSMA (green) and DAPI (blue) quantified as percentage of p-Smad2 positive cells in the fistula wall; $P = 0.0003$ (ANOVA), $P = 0.0014$ (Kruskal-Wallis), $*P = 0.0088$ (day 0 vs 7, Tukey's post hoc), $**P = 0.0090$ (day 7 vs 21, Tukey's post hoc), $***P = 0.0002$ (day 0 vs 21, Tukey's post hoc), $P = 0.0139$ (day 0 vs 21, Dunn's post hoc). **(C)** Smad2 (red), αSMA (green) and DAPI (blue) quantified as IF intensity of Smad2 in the AVF wall; $P = 0.0310$ (ANOVA), $P = 0.0619$ (Kruskal-Wallis), $*P = 0.0402$ (day 0 vs 21, Tukey's post hoc); $n = 3$ (days 0 and 21) and 4 (day 7). Four high power field images were used to acquire the mean value per animal. All data are represented as mean value \pm SEM. L, lumen; A.U., arbitrary unit. Scale bars, 20 μ m.

Figure S4

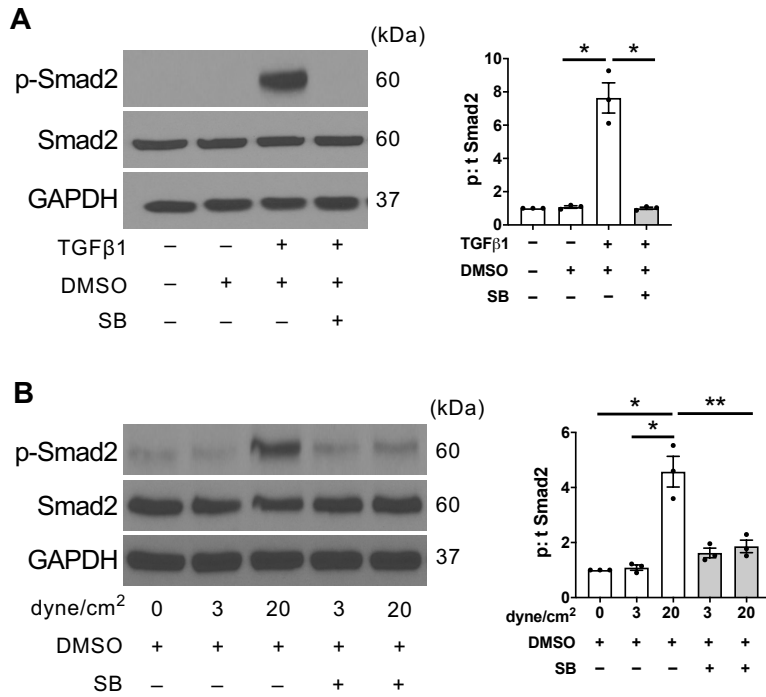


Figure S4. Activation of Smad2 by arterial shear stress is inhibited by SB431542. (A) Representative Western blot (WB) of Smad2 phosphorylation in mouse endothelial cells (EC) stimulated by TGFβ1 (5ng/ml) with and without pre-treatment with vehicle (DMSO) or SB431542, quantified with densitometry; p:t Smad2: $P < 0.0001$ (ANOVA), $P = 0.0442$ (Kruskal-Wallis), $*P < 0.0001$ (Tukey's post hoc); $n = 3$ each. **(B)** Representative WB of Smad2 phosphorylation in EC stimulated by different magnitudes of shear stress with or without pre-treatment with SB431542, quantified with densitometry; p:t Smad2: $P < 0.0001$ (ANOVA), $P = 0.0002$ (Kruskal-Wallis), $*P < 0.0001$, $**P = 0.0004$ (Tukey's post-hoc); $n = 3$ each. All data are represented as mean value \pm SEM.

Figure S5

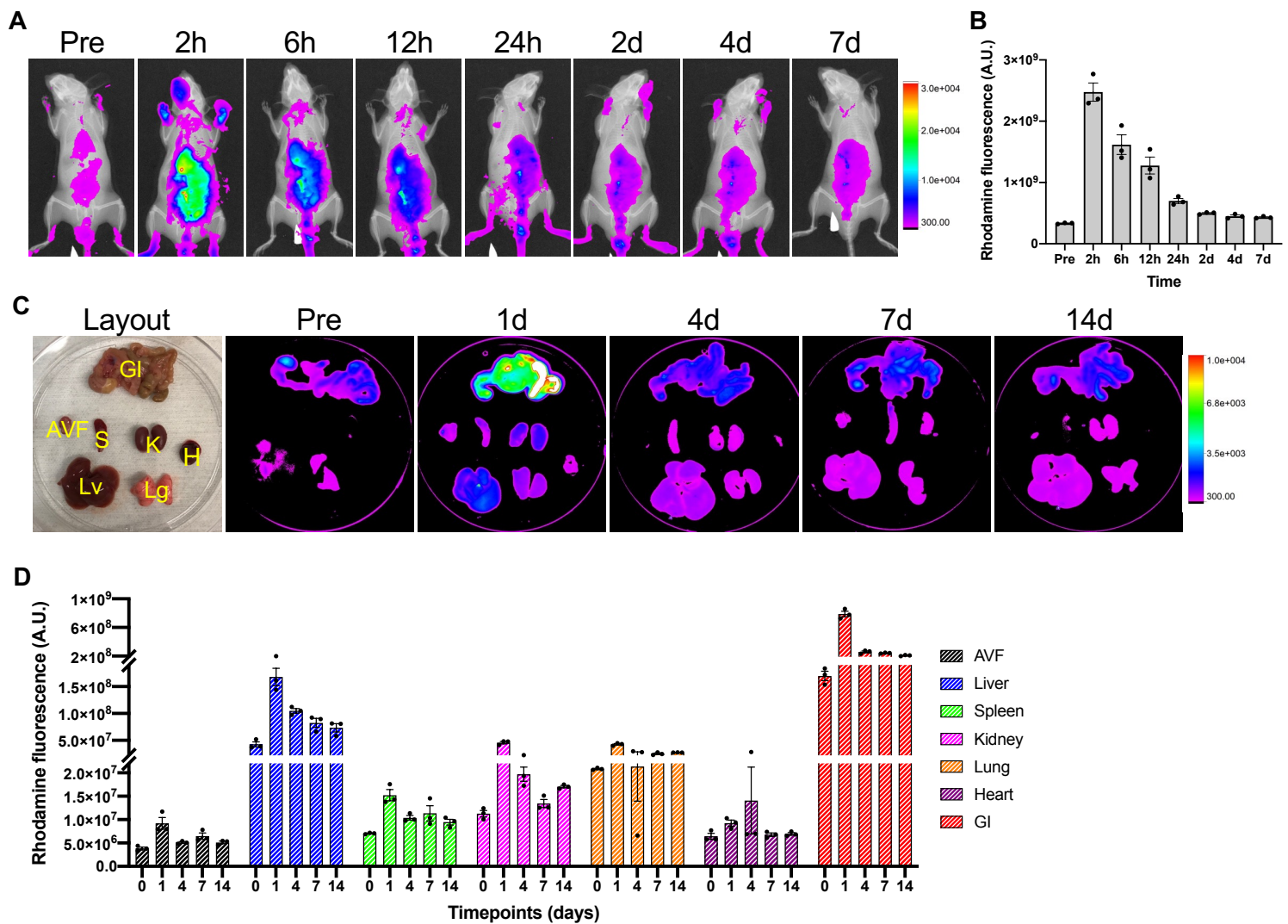


Figure S5. Enhanced retention of nanoparticles (NP) in vivo. C57BL6/J mice were administered with Rhodamine B-containing NP (NP-RhB) in pluronic gel once, immediately after arteriovenous fistula (AVF) creation and were serially observed with in vivo imaging system (IVIS). For control, IVIS imaging was obtained in mice after AVF creation but without NP-RhB administration (pre or day 0). **(A)** Representative whole-body IVIS images of mice followed to post-operative day 7, **(B)** quantified as Rhodamine B fluorescence of the whole body measured with IVIS; $n=3$ each. **(C)** Representative IVIS images of ex vivo organs harvested from mice that were followed to post-operative day 14. Layout of organs are shown on the left. **(D)** Quantification of total Rhodamine B fluorescence measured with IVIS in various organs; $n=3$ each. All data are represented as mean value \pm SEM. A.U., arbitrary unit; AVF: arteriovenous fistula, en-bloc; GI: gastrointestinal tract; H: heart; K: kidney; Lg: lung; Lv: liver; S: spleen.

Figure S6

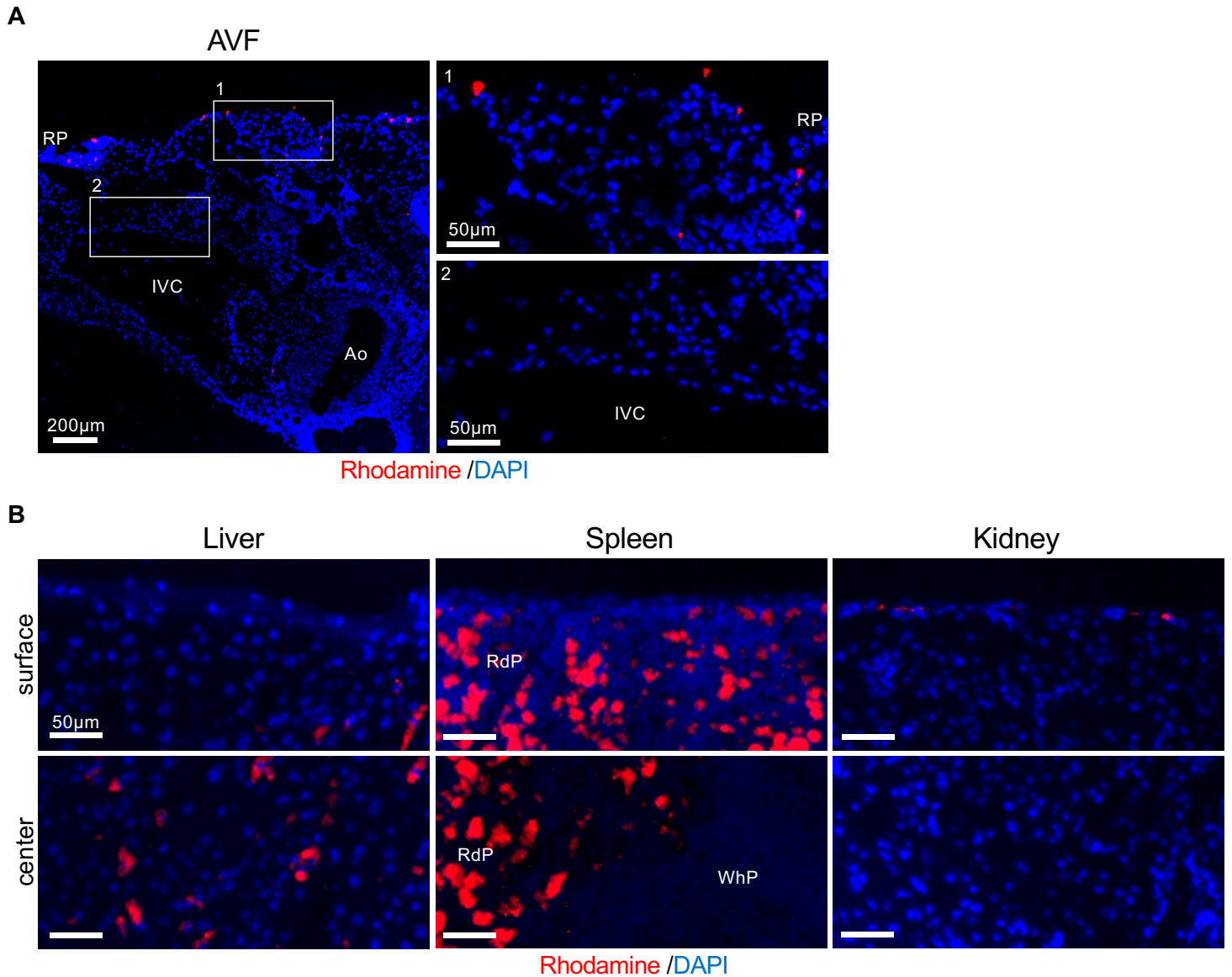


Figure S6. Immunofluorescence (IF) microscopy in mice treated with rhodamine B-containing nanoparticles in pluronic gel. C57BL6/J mice were administered with Rhodamine B-containing NP (NP-RhB) in pluronic gel once, immediately after arteriovenous fistula (AVF) creation and were harvested at day 1. **(A)** Representative IF photomicrographs of AVF sections (day 1) with Rhodamine B (RhB) fluorescence. Selected fields are shown on the right with higher magnification. Scale bars, 200 or 50 μ m. **(B)** Representative IF photomicrographs of liver, spleen and kidney sections (day 1) with RhB fluorescence. Sections including the surface (top) and the center (bottom) of each organ are shown. Scale bars, 50 μ m. *Ao*, aorta; *IVC*, inferior vena cava; *RdP*, red pulp; *RP*, retroperitoneum; *WhP*, white pulp.

Figure S7

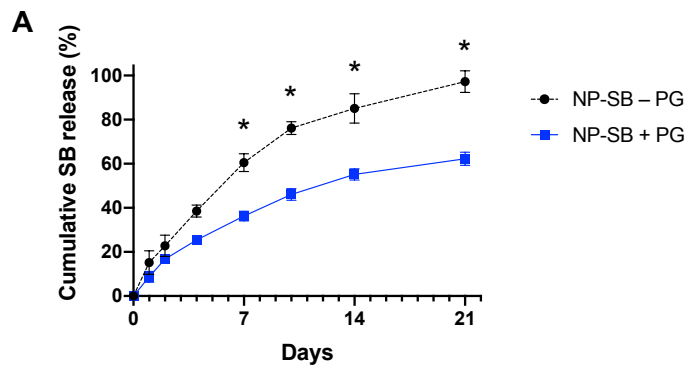


Figure S7. Controlled release of SB431542-containing nanoparticles in vitro. (A) Elution curve showing SB431542 release from NP-SB431542 (black) or NP-SB431542 in pluronic gel (blue) over 21 days in vitro; $P < 0.0001$ (ANOVA); $*P < 0.0001$ (days 7-21, Sidak's post hoc); $n = 5$ each. All data are represented as mean value \pm SEM.

Figure S8

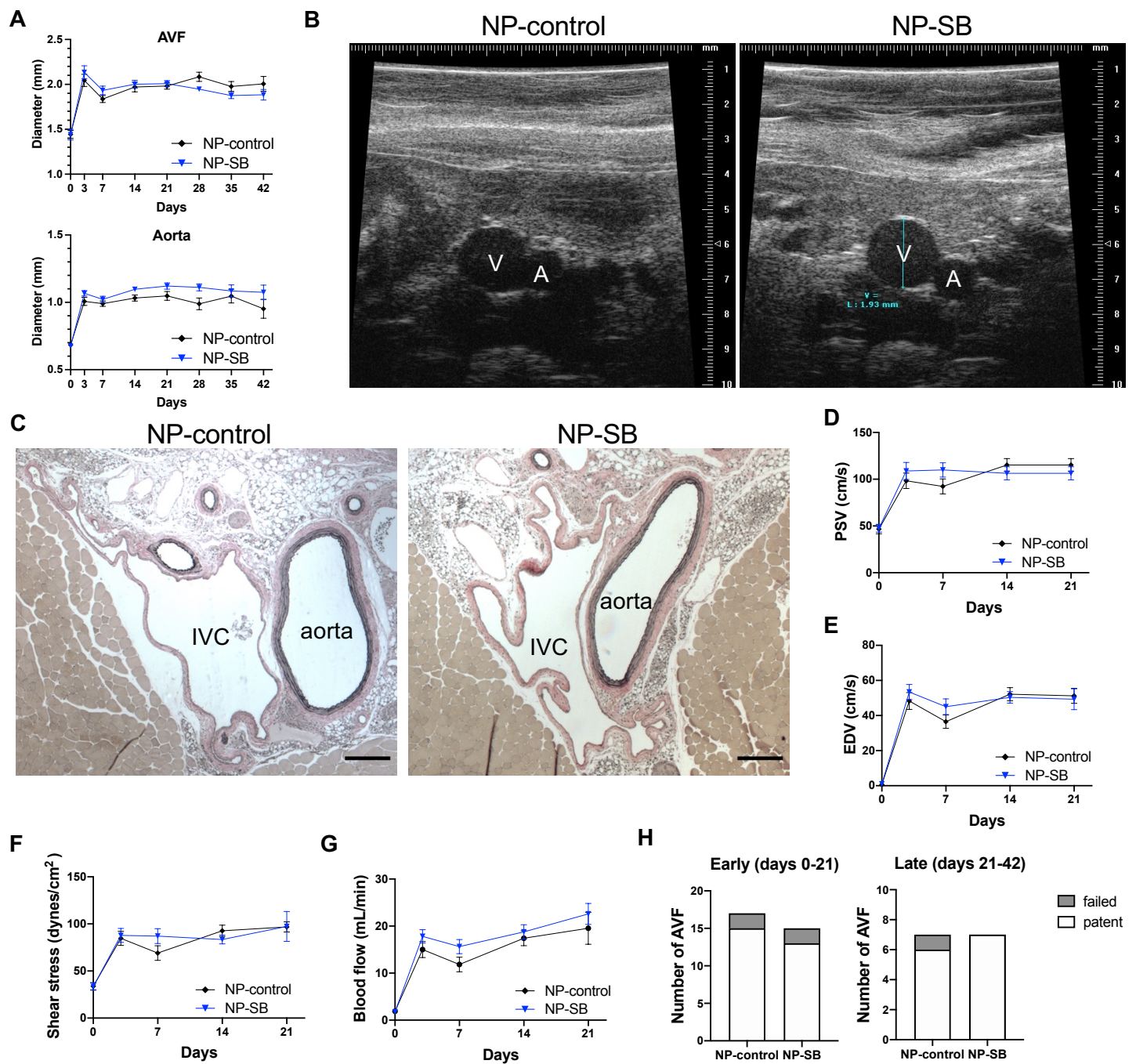


Figure S8. SB431542-containing nanoparticles (NP-SB) do not alter outward remodeling of the vessels and flow dynamics of the inflow aorta. (A) Line graph showing the inner diameter (mm) of the AVF and aorta in mice treated with NP-SB or NP-control; AVF: $P=0.7553$; aorta: $P=0.0222$ (ANOVA); $n=15$ for NP-control, $n=13$ for NP-SB. (B) Representative ultrasound images showing IVC (V) and aorta (A) treated with NP-control or NP-SB. (C) Representative photomicrographs of Van Gieson's staining of the IVC (AVF) and aorta at day 21. Scale bars, $200\mu\text{m}$. (D-G) Line graphs showing (D) peak systolic velocity (PSV), (E) end diastolic velocity (EDV), (F) shear stress and (G) blood flow of the infrarenal aorta in mice treated with NP-SB or NP-control; PSV: $P=0.6998$ (ANOVA); EDV: $P=0.4930$ (ANOVA); shear stress: $P=0.5981$; blood flow: $P=0.1472$; $n=15$ for NP-control, $n=13$ for NP-SB at day 0. (H) Bar graphs showing the number of failed and patent AVF in the early maturation phase (days 0-21) and the late failure phase (days 21-42); early: $P>0.9999$ (Fisher's exact test), $n=17$ for NP-control, $n=15$ for NP-SB; late: $P>0.9999$ (Fisher's exact test), $n=7$ each. All data are represented as mean value \pm SEM.

Figure S9

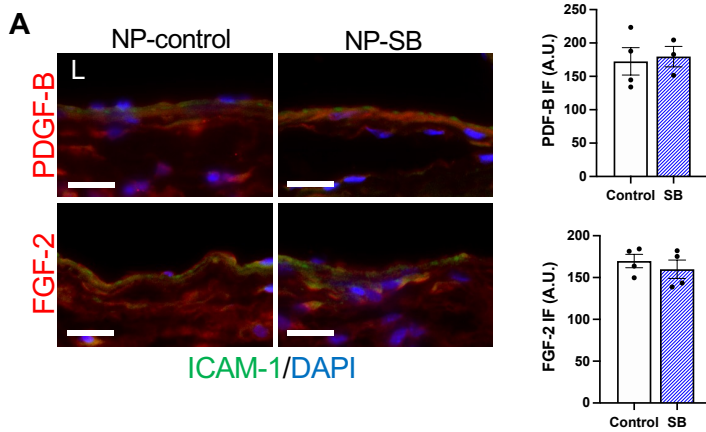


Figure S9. SB431542-containing nanoparticles (NP-SB) do not impact the expression of PDGF-B and FGF-2. C57BL/6J mice were administered with NP-SB in pluronic gel once, immediately after AVF creation (day0). Control mice were administered with unloaded nanoparticles in the same manner (NP-control). **(A)** Representative photomicrographs showing immunofluorescence (IF) of PDGF-B (red, top) or FGF-2 (red, bottom) merged with ICAM-1 (green) and DAPI (blue) in the AVF at day 7, quantified as IF intensity in the AVF wall; PDGF-B: $P=0.8046$ (t test), $P=0.8571$ (U test); FGF-2: $P=4952$ (t test), $P=0.4857$ (U test); $n=4$ for NP-control, $n=3$ (PDGF-B) or 4 (FGF-2) for NP-SB. Eight high power field images were used to acquire the mean value per animal. All data are represented as mean value \pm SEM. *L*, lumen ; *A.U.*, arbitrary unit. Scale bars, $20\ \mu\text{m}$.

Figure S10

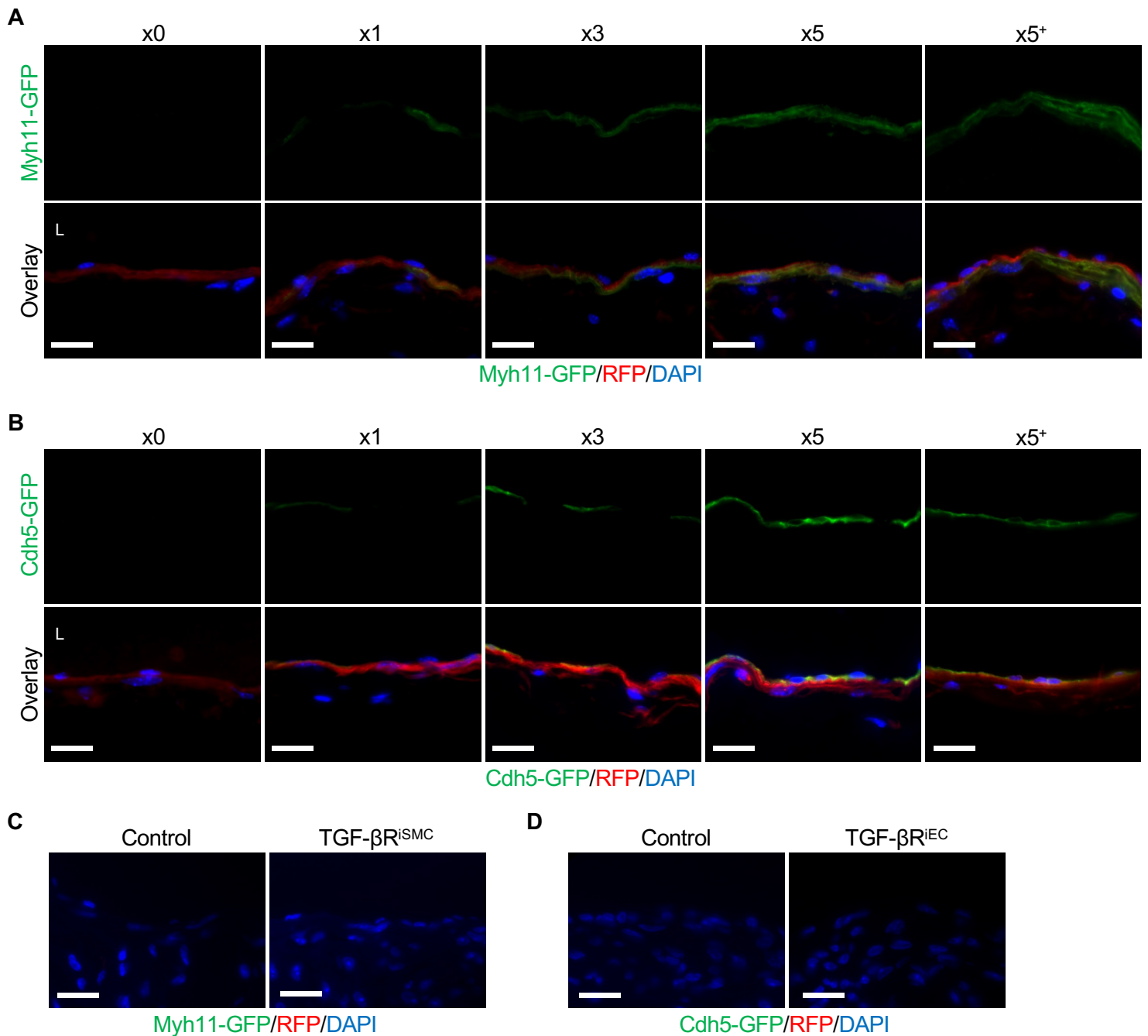


Figure S10. Confirmation of Cre recombination with tamoxifen in TGF- β receptor knock out mice. To confirm adequate Cre recombination with tamoxifen, the inferior vena cava (IVC) was harvested prior to injection (x0) or a day after the 1st, 3rd or 5th injections (x1, x3, x5, respectively). Additionally, the IVC was harvested 14 days from the start of the injections (x5⁺) when the mice would undergo AVF creation. **(A, B)** Representative immunofluorescence (IF) photomicrographs of frozen IVC sections showing GFP expression at each time point in **(A)** *Myh11-CreER^{T2}; Tgfbr2^{fl/fl}; mT/mG* mice and **(B)** *Cdh5-CreER^{T2}; Tgfbr1^{fl/fl}; Tgfbr2^{fl/fl}; mT/mG* mice. **(C, D)** Representative IF photomicrographs of paraffin-embedded AVF sections with declined mT/mG fluorescence in **(C)** *Myh11-CreER^{T2}; Tgfbr2^{fl/fl}; mT/mG* mice treated with vehicle (Control) or tamoxifen (TGF- β R^{iSMC}), and **(D)** *Cdh5-CreER^{T2}; Tgfbr1^{fl/fl}; Tgfbr2^{fl/fl}; mT/mG* mice treated with vehicle (Control) or tamoxifen (TGF- β R^{iEC}). L, lumen. Scale bars, 20 μ m.

Figure S11

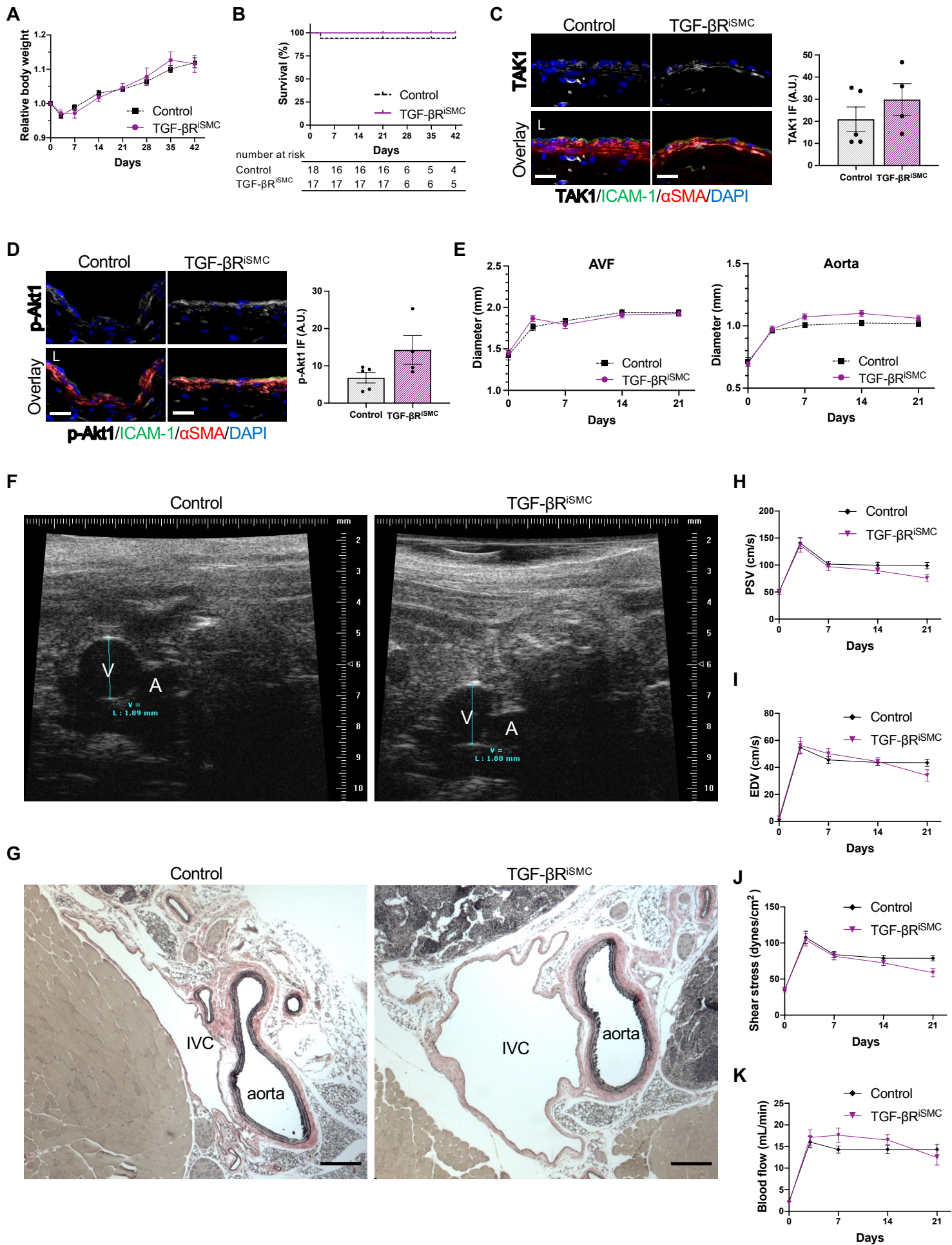


Figure S11. Inhibition of TGF- β signaling in smooth muscle cells. *Myh11-CreER^{T2}; Tgfb2^{fl/fl}; mT/mG* mice were treated with vehicle (Control) or tamoxifen (TGF- β R^{iSMC}) and underwent arteriovenous fistula (AVF) creation (day0). **(A)** Line graph showing the relative body weight up to day 42. Values are normalized by preoperative measurement. $P=0.4486$ (ANOVA); $n=16$ for control, $n=17$ for TGF- β R^{iSMC} at day 0. **(B)** Line graph showing survival, $P=0.3173$ (Log-rank); $n=18$ for control, $n=17$ for TGF- β R^{iSMC} at day 0. **(C)** Representative photomicrographs showing IF of TAK1 (white) merged with ICAM-1 (green), α SMA (red) and DAPI (blue) in the AVF wall at day 7, quantified as IF intensity of TAK1 in the media; $P=0.1905$ (*U* test); $n=5$ for control, $n=4$ for TGF- β R^{iSMC}. **(D)** Representative photomicrographs showing IF of p-Akt1 (white) merged with ICAM-1 (green), α SMA (red) and DAPI (blue) in the AVF wall at day 7, quantified as IF intensity of pAkt1 in the media; $P=0.0869$ (*t* test), $P=0.1905$ (*U* test); $n=5$ for control, $n=4$ for TGF- β R^{iSMC}. **(E)** Line graph showing the diameter (mm) of the AVF and aorta; AVF: $P=0.6461$ (ANOVA); aorta: $P=0.0132$ (ANOVA); $n=16$ for control, $n=17$ for TGF- β R^{iSMC} at day 0. **(F)** Representative ultrasound images showing IVC (V) and aorta (A) of control or TGF- β R^{iSMC} mice. **(G)** Representative photomicrographs of Van Gieson's staining of the IVC (AVF) and aorta at day 21. **(H-K)** Line graphs showing **(H)** peak systolic velocity (PSV), **(I)** end diastolic velocity (EDV), **(J)** shear stress and **(K)** blood flow of the infrarenal aorta up to day 21; PSV: $P=0.1532$ (ANOVA); EDV: $P=0.9534$ (ANOVA); shear stress: $P=0.1339$ (ANOVA); blood flow: $P=0.4546$ (ANOVA); $n=16$ for control, $n=17$ for TGF- β R^{iSMC} at day 0. Four high power field images were used to acquire the mean value per animal **(C, D)**. All data are represented as mean value \pm SEM. L, lumen; A.U., arbitrary unit. Scale bars, 20 μ m for **C, D**; 200 μ m for **G**.

Figure S12

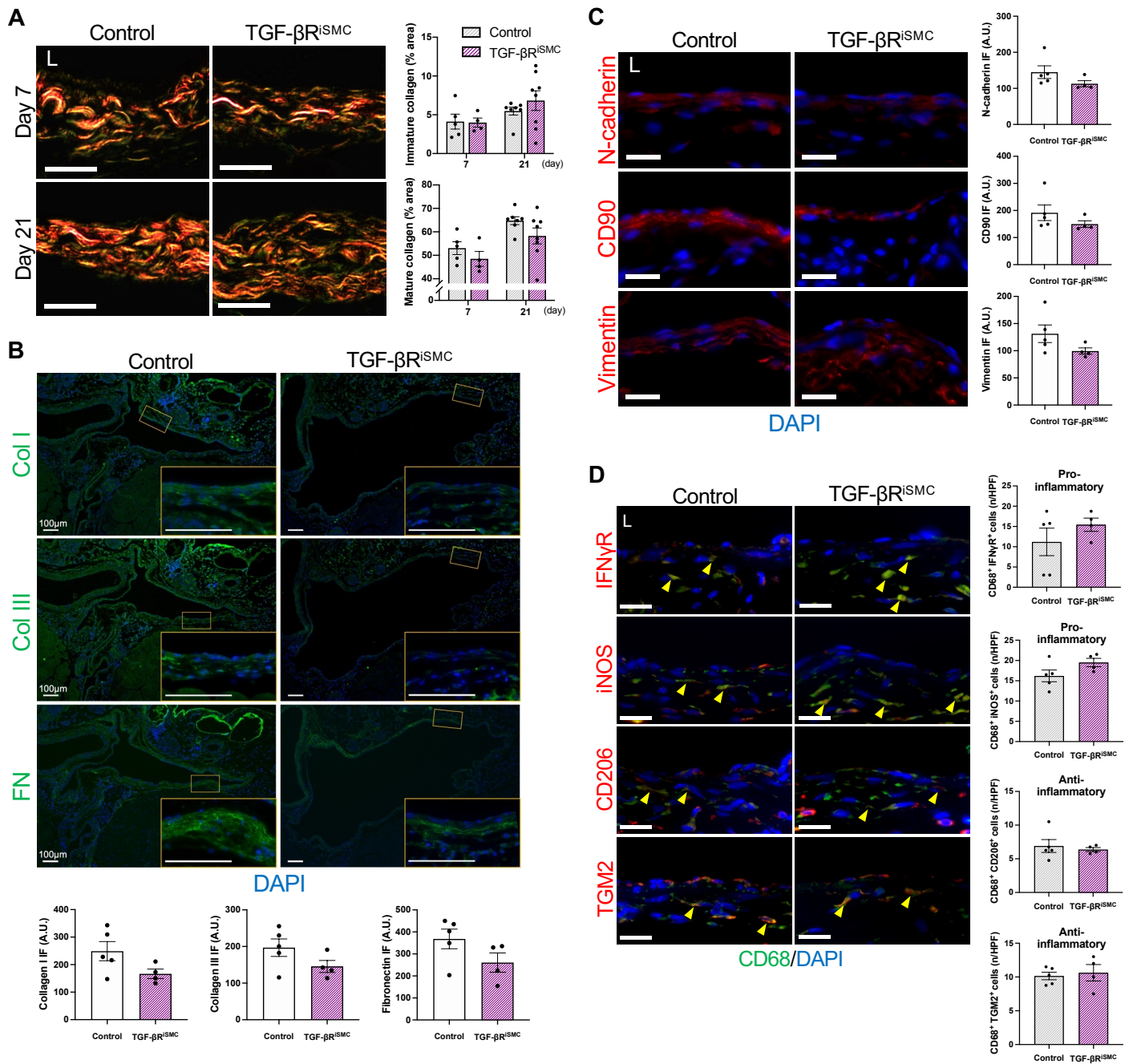


Figure S12. Inhibition of TGF- β signaling in smooth muscle cells. *Myh11-CreER^{T2}; Tgfbr2^{fl/fl}; mT/mG* mice were treated with vehicle (Control) or tamoxifen (TGF- β R^{iSMC}) and underwent arteriovenous fistula (AVF) creation (day0). **(A)** Representative photomicrographs of picosirius red staining of the AVF wall (days 7 and 21) examined under polarized light. Mature collagens appear as strongly birefringent red-orange fibers and immature collagens as weakly birefringent green fibers. Bar graphs show percentage of immature or mature collagen area within the AVF wall; immature collagen: $P=0.5677$ (ANOVA); mature collagen: $P=0.0818$ (ANOVA); $n=5$ (day 7) and $n=7$ (day 21) for control, $n=4$ (day 7) and $n=8$ (day 21) for TGF- β R^{iSMC}. **(B)** Representative photomicrographs showing immunofluorescence (IF) of collagen type I (green), collagen type III (green) or fibronectin (green) merged with DAPI (blue) in the AVF wall (day 7), quantified as IF intensity in the AVF wall; collagen type I : $P=0.0928$ (t test), $P=0.1111$ (U test); collagen type III: $P=0.1384$ (t test), $P=0.1905$ (U test); fibronectin: $P=0.1343$ (t test), $P=0.1111$ (U test); $n=5$ for control, $n=4$ for TGF- β R^{iSMC}. High-magnification images of the AVF wall shown in boxed areas are shown to the lower-right. **(C)** Representative photomicrographs showing IF of N-cadherin (red), CD90 (red) or vimentin (red) merged with DAPI (blue) in the AVF wall (day 7), quantified as IF intensity in the AVF wall; N-cadherin: $P=0.1111$ (U test); CD90: $P=0.2633$ (t test), $P=0.1111$ (U test); vimentin: $P=0.1391$ (t test), $P=0.1111$ (U test); $n=5$ for control, $n=4$ for TGF- β R^{iSMC}. **(D)** Representative photomicrographs showing IF of IFN γ R (red), iNOS (red), CD206 (red) or TGM2 (red) merged with CD68 (green) and DAPI (blue) in the AVF wall (day 7), quantified as the number of dual-positive cells in the AVF wall; CD68⁺ IFN γ R⁺: $P=0.3371$ (t test), $P=0.6032$ (U test); CD68⁺ iNOS⁺: $P=0.1221$ (t test), $P=0.0714$ (U test); CD68⁺ CD206⁺: $P=0.6535$ (t test), $P=0.9444$ (U test); CD68⁺ TGM2⁺: $P=0.7136$ (t test), $P=0.7302$ (U test); $n=5$ for control, $n=4$ for TGF- β R^{iSMC}. Four **(A, D)** or 8 **(B, C)** high power field images were used to acquire the mean value per animal. All data are represented as mean value \pm SEM. *L*, lumen; *A.U.*, arbitrary unit; *n/HPF*, number per high power field. Scale bars, 20 μ m for **A, C, D**; 100 μ m for **B**.

Figure S13

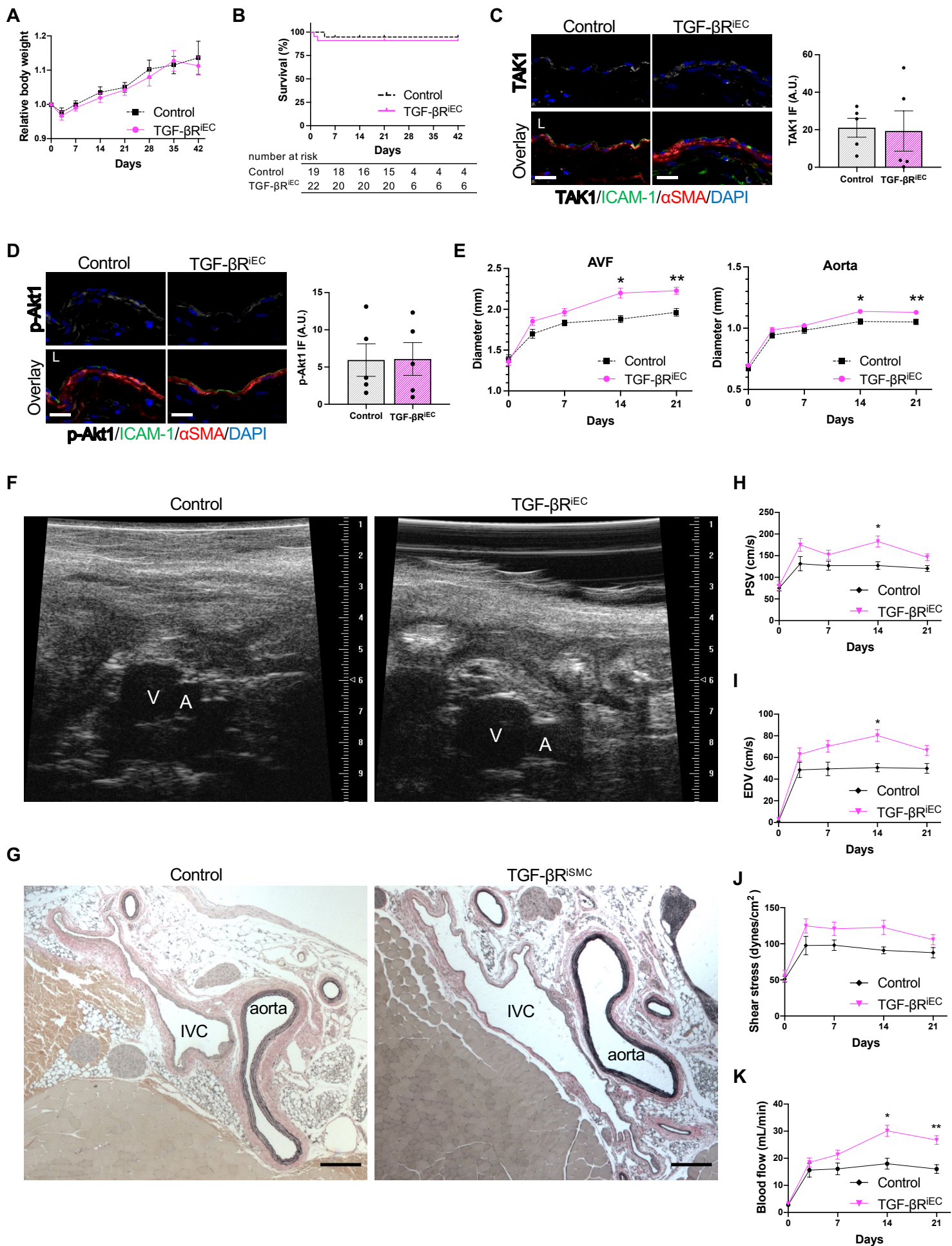


Figure S13. Inhibition of TGF- β signaling in endothelial cells. *Cdh5-Cre^{ERT2}; Tgfbr1^{fl/fl}; Tgfbr2^{fl/fl}; mT/mG* mice were treated with vehicle (Control) or tamoxifen (TGF- β R^{IEC}) and underwent arteriovenous fistula (AVF) creation (day0). **(A)** Line graph showing the relative body weight up to day 42. Values are normalized by preoperative measurement. $P=0.5715$ (ANOVA); $n=18$ for control, $n=17$ for TGF- β R^{IEC} at day 0. **(B)** Line graph showing survival, $P=0.2422$ (Log-rank); $n=19$ for control, $n=22$ for TGF- β R^{IEC} at day 0. **(C)** Representative photomicrographs showing immunofluorescence (IF) of TAK1 (white) merged with ICAM-1 (green), α SMA (red) and DAPI (blue) in the AVF wall at day 7, quantified as IF intensity of TAK1 in the intima; $P=0.8859$ (*t* test), $P=0.6905$ (*U* test); $n=5$ each. **(D)** Representative photomicrographs showing IF of p-Akt1 (white) merged with ICAM-1 (green), α SMA (red) and DAPI (blue) in the AVF wall at day 7, quantified as IF intensity of pAkt1 in the intima; $P=0.9652$ (*t* test), $P>0.9999$ (*U* test); $n=5$ each. **(E)** Line graph showing the diameter (mm) of the AVF and aorta; AVF: $P=0.0008$ (ANOVA), $*P=0.008$ (day14, Sidak's post hoc), $**P=0.0010$ (day21, Sidak's post hoc); aorta: $P=0.0031$ (ANOVA), $*P=0.0307$ (day14, Sidak's post hoc), $**P=0.0406$ (day21, Sidak's post hoc); $n=18$ for control, $n=17$ for TGF- β R^{IEC} at day 0. **(F)** Representative ultrasound images showing IVC (V) and aorta (A) of control or TGF- β R^{IEC} mice. **(G)** Representative photomicrographs of Van Gieson's staining of the IVC (AVF) and aorta at day 21. Scale bars, 200 μ m. **(H-K)** Line graphs showing **(H)** peak systolic velocity (PSV), **(I)** end diastolic velocity (EDV), **(J)** shear stress and **(K)** blood flow of the infrarenal aorta up to day 21; PSV: $P=0.0074$ (ANOVA), $*P=0.0091$ (day 14, Sidak's post hoc); EDV: $P=0.0012$ (ANOVA), $*P=0.0010$ (day 14, Sidak's post hoc); shear stress: $P=0.0074$ (ANOVA); blood flow: $P=0.0021$ (ANOVA), $*P=0.0017$ (day 14, Sidak's post hoc), $**P=0.0005$ (day 21, Sidak's post hoc); $n=13$ for control, $n=16$ for TGF- β R^{IEC} at day 0. Four high power field images were used to acquire the mean value per animal (**C**, **D**). All data are represented as mean value \pm SEM. L, lumen; A.U., arbitrary unit. Scale bars, 20 μ m for **C**, **D**; 200 μ m for **G**.

Figure S14

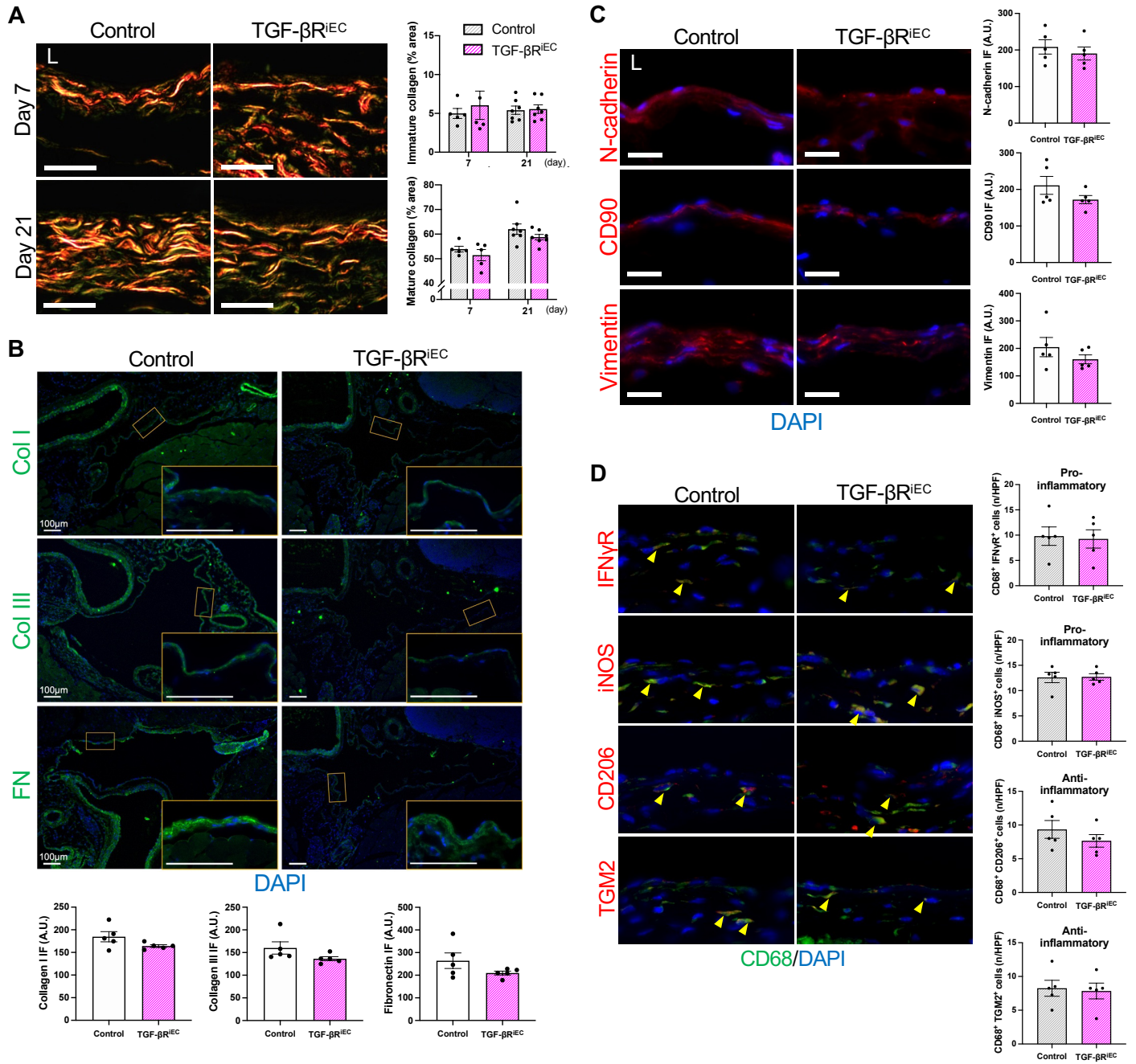
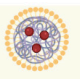


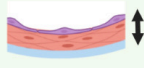
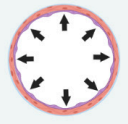
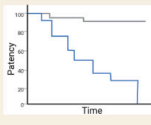


Figure S14. Inhibition of TGF- β signaling in endothelial cells. *Cdh5-CreERT²; Tgfbr1^{fl/fl}; Tgfbr2^{fl/fl}; mT/mG* mice were treated with vehicle (Control) or tamoxifen (TGF- β R^{iEC}) and underwent arteriovenous fistula (AVF) creation (day0). **(A)** Representative photomicrographs of picrosirius red staining of the AVF wall (days 7 and 21) examined under polarized light. Mature collagens appear as strongly birefringent red-orange fibers and immature collagens as weakly birefringent green fibers. Bar graphs show percentage of immature or mature collagen area within the AVF wall; immature collagen: $P=0.5221$ (ANOVA); mature collagen: $P=0.1276$ (ANOVA); $n=5$ (day 7) and 7 (day 21) for control, $n=5$ (day 7) and 7 (day 21) for TGF- β R^{iEC}. **(B)** Representative photomicrographs showing immunofluorescence (IF) of collagen type I (green), collagen type III (green) or fibronectin (green) merged with DAPI (blue) in the AVF wall (day 7), quantified as IF intensity in the AVF wall; collagen type I : $P=0.1388$ (*t* test with Welch's correction), $P=0.1508$ (*U* test); collagen type III: $P=0.0556$ (*U* test); fibronectin: $P=0.1913$ (*t* test with Welch's correction), $P=0.2222$ (*U* test); $n=5$ each. High-magnification images of the AVF wall shown in boxed areas are shown to the lower-right. **(C)** Representative photomicrographs showing IF of N-cadherin (red), CD90 (red) or vimentin (red) merged with DAPI (blue) in the AVF wall (day 7), quantified as IF intensity in the AVF wall; N-cadherin: $P=0.5149$ (*t* test), $P=0.5476$ (*U* test); CD90: $P=0.1873$ (*t* test), $P=0.3095$ (*U* test); vimentin: $P=0.2814$ (*t* test), $P=0.5476$ (*U* test); $n=5$ each. **(D)** Representative photomicrographs showing IF of IFN γ R (red), iNOS (red), CD206 (red) or TGM2 (red) merged with CD68 (green) and DAPI (blue) in the AVF wall (day 7), quantified as the number of dual-positive cells in the AVF wall; CD68⁺ IFN γ R⁺: $P=0.8359$ (*t* test), $P=0.9365$ (*U* test); CD68⁺ iNOS⁺: $P=0.9356$ (*t* test), $P=0.8333$ (*U* test); CD68⁺ CD206⁺: $P=0.3227$ (*t* test), $P=0.4206$ (*U* test); CD68⁺ TGM2⁺: $P=0.8150$ (*t* test), $P=0.8333$ (*U* test); $n=5$ each. Four **(A, D)** or 8 **(B, C)** high power field images were used to acquire the mean value per animal. All data are represented as mean value \pm SEM. *L*, lumen; *A.U.*, arbitrary unit; *n/HPF*, number per high power field. Scale bars, 20 μ m for **A, C, D**; 100 μ m for **B**.

Figure S15

Disruption of TGF- β signaling

	 Systemic	 SMC-specific	 EC-specific
Remodeling			
Wall thickness 	↘	→	↘
Vessel dilation 	→	→	↑
Outcome			
AVF patency 	→	→	↑

→ : no change ↘ : trend towards decrease ↑ : significant increase

Figure S15. Summary of the effect of pharmacological pan-inhibition and cell type-specific inhibition of TGF- β signaling on AVF maturation.